ANALYTICAL LETTERS, 31(13), 2209-2229 (1998)

NEAR-IR ELECTROGENERATED CHEMILUMINESCENCE OF TRICARBOCYANINE DYES IN MICELLAR SYSTEMS

Sang Kwon Lee and Allen J. Bard*

Department of Chemistry and Biochemistry, The University of Texas at Austin, Austin, Texas 78712

ABSTRACT

Two tricarbocyanine near-IR dyes containing the same (dimethyl naphthalindole) heterocyclic nuclei, IR144 and IR125, were studied in organic solvents, in water, and in the presence of certain surfactants. The anodic oxidation of IR144 produces electrogenerated chemiluminescence (ECL) in the presence of tri-n-propylamine as a coreactant in sodium dodecyl sulfate surfactant solution or in MeCN/DMSO (2:1 v/v) solution. The one-electron oxidation of IR144 generated the corresponding fairly stable radical cation at +0.48 V vs Ag/AgCl in MeCN/DMSO (2:1). In the micelle system, the potential was shifted to a more positive potential, +1.1 V vs Ag/AgCl, as found by

differential pulse voltammetry. The ECL intensity for IR125 was much weaker than that of IR144, and the potential did not change in water or surfactant solution. The absorption spectra indicated extensive dimerization for IR144 in aqueous solution, while IR125 showed little evidence of dimerization. For IR144, the fluorescence intensity in water decreased dramatically when compared to both organic solvents MeOH and MeCN. In all the aqueous surfactant solutions, the fluorescence intensity is partially restored. These micelle ECL reactions should be useful in the design of new labels for ECL applications.

INTRODUCTION

The $Ru(bpy)_3^{2+}$/tri-n-propylamine (TPrA) system has been used in aqueous solution for electrogenerated chemiluminescence (ECL) applications. However, the need for new labels to allow simultaneous analysis and internal referencing has prompted us to consider emitters other than $Ru(bpy)_3^{2+*}$ as ECL labels. Requirements of new labels for ECL[1] are (i) the emission wavelength should be distinct from that of $Ru(bpy)_3^{2+}$, (ii) the emitter must be soluble in aqueous solution, (iii) the electrochemical oxidation or reduction should proceed within the relatively narrow potential range imposed by the oxidation and reduction of H_2O, and (iv) the oxidized or reduced intermediate must react with the electrogenerated coreactant intermediate, allowing formation of the excited state. In addition, the emitter should have high fluorescence efficiency, and the radical ions should also be stable and should not dimerize.

Considering the above points, some of near-infrared (NIR) dyes are prime candidates. We have shown that the heptamethine cyanine dye (HMC), an NIR dye, produces near-IR ECL in the presence of TPrA in MeCN[2]. Since most of the known NIR dyes, including the polymethine chain, are ionic molecules, they are insoluble in nonpolar organic solvents, but they are soluble in most polar

organic or aqueous solvents. Due to their hydrophobic nature, these NIR dyes tend to form aggregates when the hydrophobicity of the solvent decreases, especially in an aqueous environment. These structural changes in water degrade fluorescence efficiencies, but the problem can be solved by deaggragation through a micellar system. Micellar effects on the fluorescence behavior of these dyes can greatly enhance the emission intensity[3].

We report the spectroscopic properties and oxidative electrochemistry of some NIR dyes and their ECL in the presence of TPrA through micellar systems. Micelles have been used in applications of colloidal redox electrochemistry[4] and are of interest in micellar catalysis and micellar models of biological membranes[5]. Because micelles are dynamic aggregates of amphiphilic molecules they possess regions of hydrophilic and hydrophobic character[6]. The interactions that are operative between soluble substances and host micelles include electrostatic attractions, surface adsorption, pseudophase extraction[7], and substrate/amphiphilic coassembly to yield a unique micelle composition[8]. The specific nature of the interaction between a soluble species and the host micelle governs the effect of the micellar microenvironment on the behavior of the substrate.

In the present study, we show that the NIR dye does produce ECL even in a micellar system, and we examine the microenvironment effects of micelles on the spectroscopic and electrochemical behaviors of some NIR dyes. Sodium dodecyl sulfate, cetyltrimethylammonium bromide, and Triton X-100 were used as the representatives of anionic, cationic, and neutral micelles, respectively.

EXPERIMENTAL

Chemicals

Water-soluble surfactants, sodium dodecyl sulfate (SDS, Aldrich), cetyltrimethylammonium bromide (CTAB, Alfa Products), and TritonX-100

(Fluka) were used as received. Tri-*n*-propylamine (TPrA, 98%, Aldrich, Milwaukee, WI) was also used as received. Tetra-*n*-butylammonium hexafluorophosphate ($TBAPF_6$, SACHEM, Austin, TX) was recrystallized from $EtOH/H_2O$ (4:1) three times and dried at 100°C before use. Acetonitrile (MeCN, Burdick and Jackson, UV grade) and dimethylsulfoxide (DMSO, GR grade) were used as received after being transported unopened into an inert atmosphere drybox (Vacuum Atmospheres, Los Angeles, CA).

The near-infrared dyes (Fig. 1) IR-125 (indocyanine green, $C_{43}H_{47}N_2NaO_6S_2$, laser grade) and IR-144 ($C_{56}H_{73}N_5O_8S_2$, laser grade) were obtained from Acros Organics (New Jersey). Stock solutions of 10^{-3} M IR-125 or IR144 in MeCN/DMSO (2:1, v/v) were used to prepare test solutions. The solutions containing surfactants were maintained well above their critical micelle concentration (CMC)[6]. Deionized water (18 MΩ) from a Millipore Milli-Q system and phosphate buffer (pH 7.3) were used throughout. The water was deaerated with N_2 for 20 min immediately before the preparation of IR-125 solutions to prevent decomposition of the dye by oxygen.

All solutions for UV/vis, fluorescence, electrochemical, and ECL studies in organic solvents were prepared in a glovebox (Vacuum Atmospheres) under a helium atmosphere and sealed in air-tight cells.

Apparatus and Procedures

Some of the ECL and electrochemical measurements in surfactants were performed on an ORIGEN I analyzer (IGEN, Gaithersburg, MD), which integrates a photometer, potentiostat, electrochemical cell, and a means for fluid and sample handling. The sequence of operations is controlled by an IBM PS/2 model 25 PC. The cell utilizes a conventional three-electrode setup and is arranged as a flow-through system (Fig. 2). The working and counter electrodes are 0.30 cm diameter platinum disks, and the Ag/AgCl reference electrode is located in a compartment beside the flow path downstream from the cell.

IR144

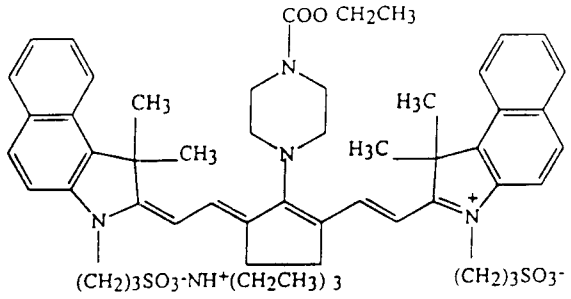

IR125

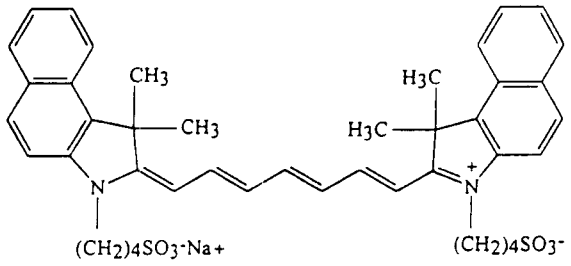

FIG. 1. Structures of the tricarbocyanine dyes used.

A charge-coupled device (CCD) camera (Photometrics CH260), cooled to below −130°C and interfaced to a PC, was used to obtain ECL spectra in organic solutions. The camera was focused on the output of a grating spectrometer (Holographics, concave grating and 1 mm entrance slit). The CCD camera and general configuration of the spectra acquisition have been described previously[9].

Cyclic voltammograms were recorded on a Model 660 electrochemical workstation (CH Instruments, Memphis, TN). The working electrode consisted of an inlaid platinum disk (1.5– or 2.4–mm diameter) that was polished on a felt

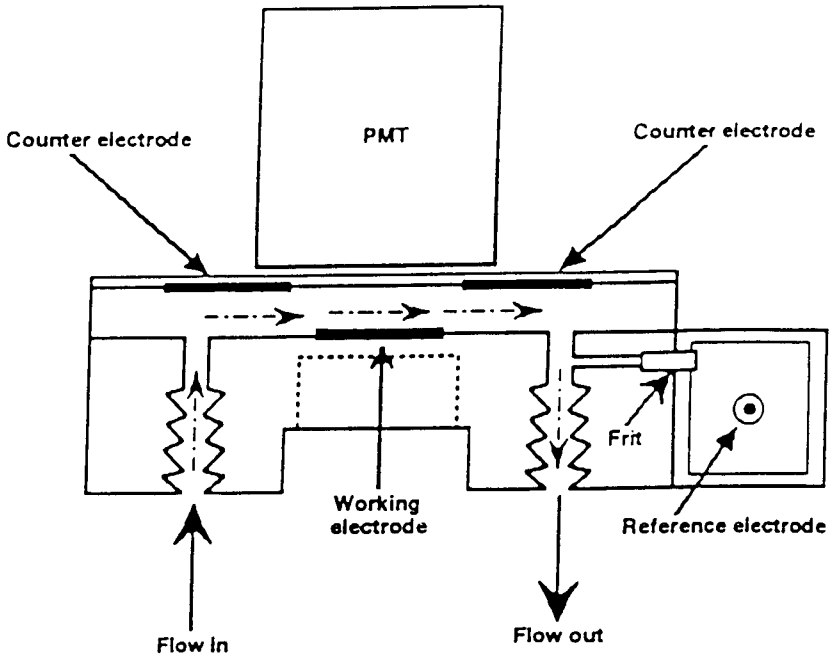

FIG. 2. Schematic diagram of the ORIGEN I electrochemical analyzer.

pad with 0.05 μm alumina (Buehler) and sonicated in absolute EtOH for 1 min before each experiment. A platinum wire served as a counter electrode. A silver wire served as a quasi-reference electrode and was referenced to a Ag/Ag electrode ($Ag/AgBF_4$) in MeCN for the determination of redox potentials. A silver/silver chloride (Ag/AgCl) electrode served as a reference electrode in aqueous surfactant solutions.

UV/vis spectra were acquired on a Milton Roy Spectronic 3000 array spectrophotometer. Fluorescence spectra were obtained using a SLM Aminco SPF-500 spectrofluorometer. The calculation of the fluorescence quantum yield has been described previously[2].

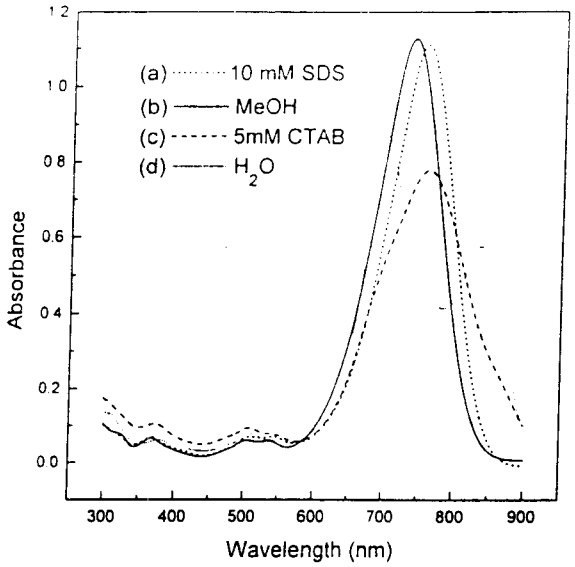

FIG. 3. Absorption spectra of 1.0×10^{-5} M IR144 in (a) aqueous 0.1 M SDS, (b) MeOH, (c) aqueous 5.0×10^{-3} M CTAB, and (d) H_2O.

RESULTS AND DISCUSSION

Absorption Spectra

Absorption spectra provide information about solvation effects and aggregation. Absorption spectra for IR144 in different media are shown in Figure 3. IR144 tends to form aggregates and these affect the absorption spectra depending upon the hydrophobicity of the environment. The absorption spectrum for IR144 in MeOH, where IR144 exists predominantly in the monomer form, shows a single absorption band with a maximum at 741 nm. In pure water, the spectrum shows two bands. The band at 701 nm is associated with a dimer or other higher-order aggregate. Solutions of NIR dyes in aqueous systems are

known to exhibit an absorption band different from that observed in less concentrated solutions or in organic solvents[10]. Other NIR dyes also display this type of behavior in water, where they tend to form dimers or higher aggregates because of the strong dispersion forces associated with the high polarizability of the polymethine chain. The absorption maximum for the dimer usually appears at a shorter wavelength than the monomer band. In aqueous solution, NIR dye dimer formation depends on concentration, with no significant dimerization observed at concentrations below 10^{-5} M. At concentrations above 10^{-4} M, higher-order aggregates, which have been identified as H and J aggregates, are observed in aqueous solutions[10,11]. The H aggregates are characterized by an absorption maximum at a shorter wavelength, while the J aggregates show an absorption maximum at a longer wavelength than the monomer band. The H and J aggregates have head-to-head and head-to-tail stack structure, respectively. The absorption band for IR144 in water at 835 nm is not associated with J aggregates, since it appears even at very low solution concentrations (0.5 μM) with deaeration just before preparation.

In Table I, the wavelength of the absorption maxima and the molar absorptivity at λ_{max} for IR144 and IR125 are presented in the solvent systems investigated. The addition of surfactants above the CMC to the aqueous solvent produced a red shift when compared to the absorption maxima observed in water. The spectra in SDS, CTAB, and Triton X-100 micellar solutions are close to the spectrum in MeOH. The shift in the absorption maxima to longer wavelengths by the addition of surfactants above the CMC to the aqueous solvent implies effective partitioning of these dyes into the hydrophobic cavity of the anionic and nonionic micelles, where the dye is shielded from the water, since solvents of increasing nucleophilicity cause a blue shift in the absorption maximum[3a]. No differences in the absorption spectra for IR125 and IR144 in H_2O and D_2O were observed. Thus we conclude that in pure aqueous solution IR144 exists as a solvated aggregate, which can be dissociated to the monomer by addition of surfactants that form micelles.

Table 1

Adsorption Maxima and Molar Extinction Coefficients for IR144 and IR125 in Different Solvents and Aqueous Surfactant Solutions

Solvent	IR144		IR125	
	$\lambda_{ab.max}$ (nm)	ε $10^{-5}(cm^{-1}\ M^{-1})$	$\lambda_{ab.max}$ (nm)	ε $10^{-5}(cm^{-1}\ M^{-1})$
MeCN/DMSO	738	1.21	793	2.00
MeOH	741	1.12	786	1.94
H_2O	701	0.85	781	2.05
H_2O/SDS	755	1.10	791	1.70
H_2O/CTAB	759	0.78	798	1.94
H_2O/TritonX-100	758	1.08	798	1.95

With IR125, no apparent dimer or aggregation was observed, since the general shapes of the spectra in water and MeOH were similar. The only difference was a slight blue shift in the absorption maximum in water. The lack of aggregation of this dye in an aqueous solvent most likely arises from the negatively charged sulfonate groups, providing the dye with a better solvation sphere[3a].

Fluorescence Spectra

Even larger solvent effects are found in the fluorescence of these compounds. Figure 4 shows the fluorescence spectra for IR144 in (a) MeOH, (b) aq. CTAB, (c) aq. SDS, and (d) H_2O. For IR144, the fluorescence intensity in water is much smaller than that in MeOH. Addition of surfactant restores a large part of the fluorescence intensity. The fluorescence maxima and quantum efficiencies for IR144 and IR125 are given in Table 2. The spectra for IR125 show a decrease in the emission intensity in water when compared to MeOH with

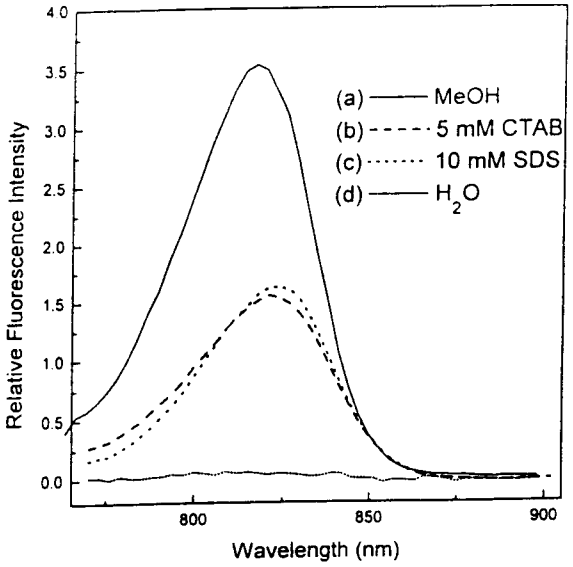

FIG. 4. Fluorescence spectra of 5.0×10^{-6} M IR144 in (a) MeOH, (b) 5.0×10^{-3} M CTAB, (c) 0.1 M SDS. and (d) H_2O at each $\lambda_{ab.max}$.

an associated blue shift in the fluorescence maximum. In the surfactant solutions. the fluorescence maxima shifted to longer wavelengths when compared to water. The relative intensities for Triton X-100 and SDS solutions are slightly higher when compared to H_2O. In the case of D_2O, the relative intensity for IR144 is similar to that in H2O, while the intensity for IR125 was much higher in D_2O compared to H_2O. The difference can be explained by the more rigid and planar structure of IR125 that gives rise to lower rates of the internal conversion processes due to a reduced number of vibrational degrees of freedom[3a]. The structure of IR144 includes a bridging group within the heptamethine chain, while IR125 does not have a bridging group. The conformationally rigid polymethine chain in NIR dyes leads to fewer vibrational degrees of freedom when compared to the visible fluorescence dyes. For visible fluorescence dyes,

Table 2

Fluorescence Maxima and Quantum Efficiency Molar Extinction Coefficiencies for IR144 and IR125 in Different Solvents and Surfactant Solutions

	IR144		IR125	
Solvent	$\lambda_{fl,max}$ (nm)	Φ_{fl}	$\lambda_{fl,max}$ (nm)	Φ_{fl}
MeCN/DMSO	820	0.07	835	0.13[a]
MeOH	818	0.06	830	0.04
H_2O	---	---	---	0.01
D_2O	---	---	815	0.07
SDS	825	0.07	835	0.02
CTAB	820	0.06	835	0.03
TritonX-100	823	0.07	838	0.03

[a] Data from results of R. C. Benson and H. Kues[12].

internal conversion is negligible because of the large energy gap between electronic levels involved in the transition. In the NIR dyes, smaller energy gaps between electronic levels lead to higher rates of internal conversion.

The deaggregation effect by addition of surfactants to form an aqueous micellar system can account for the enhancement of fluorescence intensity when compared to water. Additional factors in the nonradiative rates, such as photoisomerization at the polymethine chain[13], internal conversion[3a], and solvent-dependent effects,[3c,13] may play a role. The decrease in the nonradiative rates for NIR dyes in the micelle solutions, when compared to pure water, is the result of changes in the microenvironment associated with the interior of the micelle[3a]. These changes include a higher viscosity, lower dielectric constant and polarity, poorer hydrogen bond donor capabilities, and better nucleophilicity when

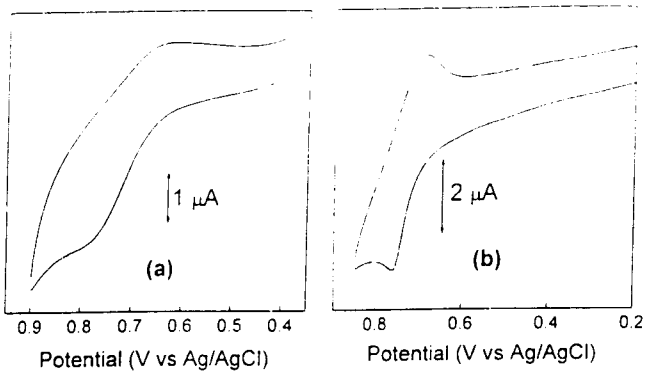

FIG. 5. Cyclic voltammograms of 1.0×10^{-3} M IR125 in (a) H_2O and (b) 0.1 M SDS. Scan rate, 0.1 V/s; Pt electrode diameter, 1.5 mm; electrolyte, 0.1 M sodium phosphate buffer, pH 7.3.

compared to the interstitial solution. The fluorescence lifetimes for NIR dyes demonstrate negligible dependence on solution viscosity, indicating that cis/trans photoisomerization is not a major nonradiative path for these tricarbocyanine dyes[3a].

Electrochemistry

Both IR144 and IR125 are anionic in water and probably in MeCN; IR144 will be represented as A– in the following discussion. IR125 is sufficiently soluble in water to show satisfactory electrochemistry in the absence of surfactant (Fig. 5a). IR144 is only very slightly soluble in water, so clean electrochemistry could not be observed without surfactant, and the very small waves seen with surfactant in water are less distinct than the well-developed waves in nonaqueous media (Fig. 6). The oxidation of 0.4 mM IR144 (MeCN/DMSO, 2:1, 0.1 M $TBAPF_6$) at a scan rate, ν, of 0.2 V/s shows a reversible one-electron oxidation wave probably corresponding to generation of the radical A• at +0.48 V vs Ag/AgCl. The substitution of a dimethylindole

group at the heterocyclic nuclei to a naphthalindole group in IR144 tends to make the molecule easier to oxidize, compared, for example, to the related heptamethine cyanine dye, $HMC^{\bullet}$; the oxidation of HMC^{+} which has a dimethylindol group on the heterocyclic nucleus occurs at + 0.55 V vs SCE^{2}. IR144 undergoes a second, chemically irreversible oxidation at +0.79 V vs Ag/AgCl. This corresponds to the second oxidation of HMC^{+}.

A cathodic voltammetric wave was also observed in the aprotic solvent for IR144 at −0.88 V vs Ag/AgCl. The instability of the reduced form of IR144 prevented efficient generation of ECL via annihilation of the neutral radical $A^{\bullet}$ and dianion radical $A^{\bullet 2-}$. However, the good stability of $A^{\bullet}$ suggested that oxidation in the presence of a coreactant could produce ECL, as described below.

Cyclic voltammograms of 1.0 mM IR144 in 50 mM NaCl and 0.1 M SDS aqueous solutions are shown in Fig. 6b and 6c. The first oxidation wave observed at 0.62 V vs Ag/AgCl shows a small one-electron quasi-reversible oxidation. A second irreversible oxidation wave is observed at 0.86 V vs Ag/AgCl and probably corresponds to the one-electron oxidation of $A^{\bullet}$ to A^{+} as in MeCN/DMSO. The cyclic voltammogram for 0.2 mM IR144 with 0.1 M TPrA as coreactant in the aqueous SDS system is shown in Figure 6d. The irreversible wave is due to the direct oxidation of TPrA at the electrode. The oxidation wave of TPrA is superimposed on the second oxidation wave of IR144, but does not overlap appreciably with the first oxidation wave. The second oxidation wave of IR144 is not seen in this scan because of its low relative concentration, and the catalytic reaction between A^{+} and TPrA. Note that the oxidation of TPrA typically merges with the background oxidation of water. However, in surfactant solution, the positive shift of the oxidation of water, because of surfactant adsorption on the electrode, allows a larger anodic region to be examined.

The diffusion coefficient, D_{ob}, is a measure of the association of electroactive molecules with the surfactant and micelles. A plot of the anodic

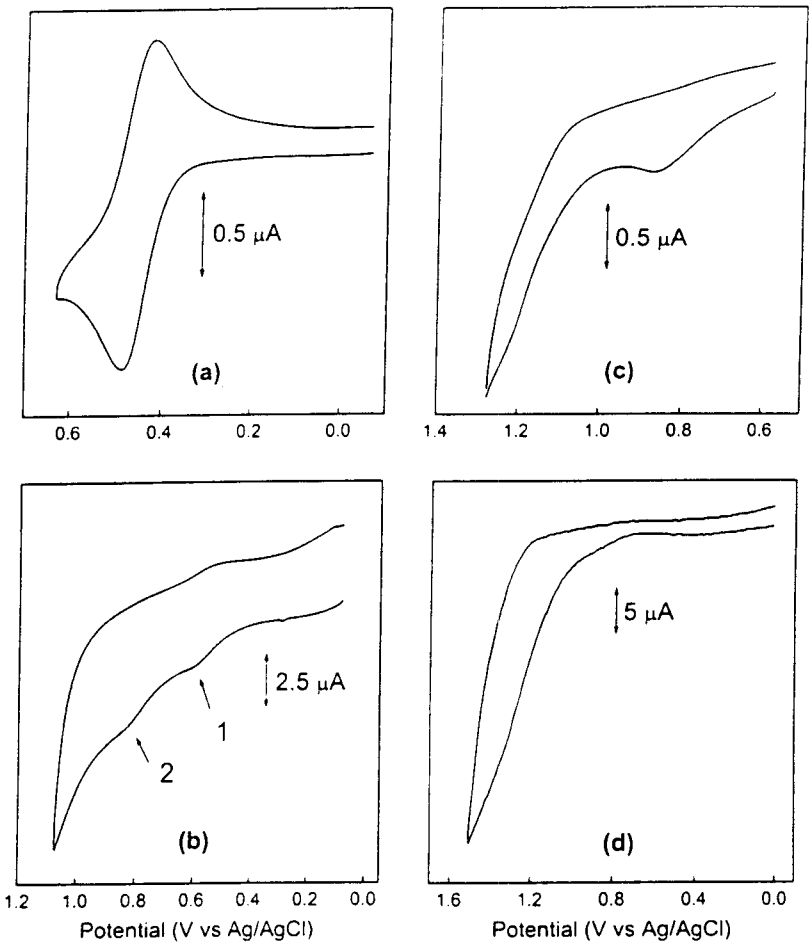

FIG. 6. Cyclic voltammograms of (a) 4.0×10^{-4} M IR144 in MeCN/DMSO (2:1 v/v); scan rate, 0.2 V/s; electrolyte, 0.1 M $TBAPF_6$; (b) 1.0×10^{-3} M IR144 in 0.05 M SDS; scan rate, 0.2 V/s; (c) 1.0×10^{-3} M IR144 in 0.05 M SDS; scan rate, 0.05 V/s, electrolyte, 0.1 M NaCl; sodium phosphate buffer, pH 7.3; and (d) 2.0×10^{-4} M IR144 and 0.1 M TPrA in 0.1 M SDS; scan rate, 0.05 V/s; 0.1 M sodium phosphate buffer, pH 7.3.

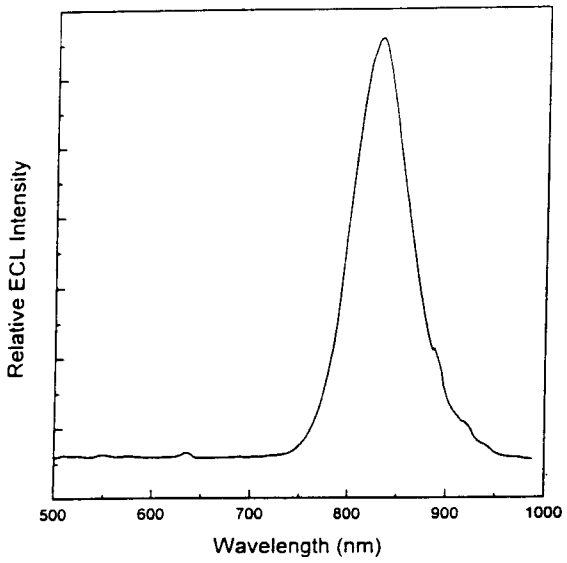

FIG. 7. ECL spectrum of 2.0 x 10^{-4} M IR144 with 6.0 x 10^{-2} M TPrA in MeCN/DMSO (2:1 v/v). The potential was stepped from 0 to 1.4 V, and the exposure time was 15 min. Electrolyte, 0.1 M $TBAPF_6$.

peak current for the oxidation of 1.0 mM IR144 versus $v^{1/2}$ is linear and intersects the origin, indicating that the electrode reaction is diffusion-controlled in the presence of surfactant. This suggests that the electrochemically active species in the presence of SDS is micelle-solubilized IR144 in the bulk solution, since the solubility of IR144 is higher in SDS than in aqueous solution. Micelle incorporation of IR144 is also evident from the decreased diffusion coefficient for IR144 in 0.1 M SDS. Typically, the values of D_o in aqueous solution for molecules of this size are 10^{-5}–10^{-6} cm^2 s^{-1}, while D_o, calculated from the slope of the plot of scan rate dependence (Fig. 7)[14], was 8.7 x 10^{-8} cm^2 s^{-1} in 0.1 M SDS and 50 mM NaCl solution. The diffusion coefficient value was. The

decrease in D_o agrees with previous results of other studies involving association with surfactants and in micellar assemblies[15-17].

However, with IR125, an oxidation wave was observed at +0.76 V vs Ag/AgCl due to its higher solubility in water (Fig. 5a). Figure 5b shows a small but well-defined wave for the oxidation of 1 mM IR125 at +0.76 V vs Ag/AgCl in SDS surfactant above the CMC. No difference in the oxidation peak potentials in aqueous and SDS solutions was observed. In general, the presence of micellar aggregates creates a microdomain with which an organic compound interacts on the basis of electrostatic and hydrophobic forces. The organic compounds can be grouped according to different interactions with ionic micelles as follows: (1) nonassociating compounds, (2) compounds partitioned between an aqueous phase and a micellar pseudophase, (3) completely associated compounds. As shown by the spectroscopic and the electrochemical properties, IR125 is included in the second group above, and IR144 is presumably included in the third.

Electrogenerated Chemiluminescence

Although the reduced forms of these species are not stable, even in aprotic solvents, and thus the electron transfer annihilation to produce excited states cannot be carried out, ECL can be obtained by the use of a coreactant like TPrA in a purely oxidative mode. Figure 7 shows the ECL spectrum for IR144 (0.2 mM IR144/0.1 M TPrA) with the potential repeatedly stepped from 0 to +1.4 V (pulse width, 0.2 s) in MeCN/DMSO (v/v, 2:1). The observed emission intensity at the platinum electrode suggested a high ECL efficiency. The relative ECL efficiency (ϕ_{ECL}) for the $IR144^-$/TPrA system was 0.17, compared to that for the $Ru(bpy)_3^{2-}$/TPrA system, taken as unity, at the same concentration. The emission spectrum was centered around 825 nm, slightly shifted to longer wavelengths compared to the fluorescence (Fig. 4) probably because of an inner-filter effect. Because the ECL solution is more concentrated than the solution used for the fluorescence measurement, the shorter emission wavelengths are

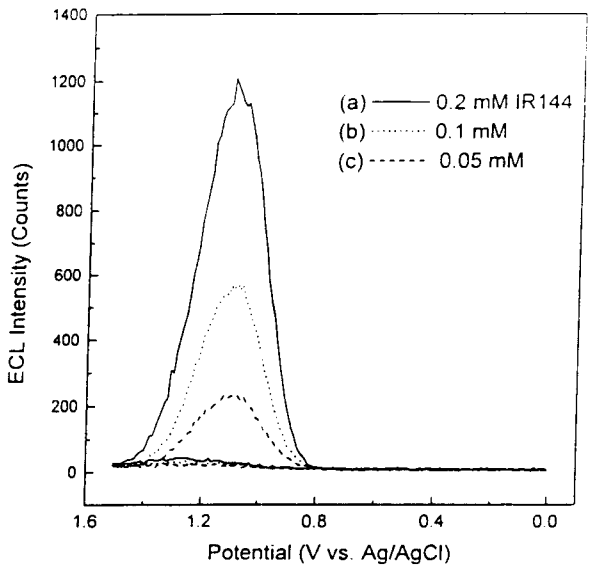

FIG. 8. ECL emission–potential transient of (a) 2.0×10^{-4}, (b) 1.0×10^{-4}, and (c) 5.0×10^{-4} M IR144 and 0.1 M TPrA in 0.1 M SDS solution. Scan rate. 0.05 V/s; 0.1 M sodium phosphate buffer. pH 7.3.

absorbed more strongly in passage through the IR144 solution as previously seen with HMC^{-}.[2]

ECL can also be produced in an aqueous solution in the presence of surfactant to increase solubility and emission efficiency. Figure 8 shows the ECL of different concentrations of IR144 with 0.1 M TPrA as coreactant (10 mM SDS, 0.1 M sodium phosphate buffer. pH 7.3) during a potential sweep from 0 V to +1.5 V (scan rate, 0.05 V/s). ECL measurements and electrochemistry in surfactant solutions were carried out with the ORIGEN I analyzer which measures total light output with a photomultiplier tube. The maximum ECL emission occurred at +1.1 V with the onset of ECL appearing at about +0.8 V with TPrA as coreactant. Note that because of considerable resistance between

reference and working electrodes in the flow cell in the ORIGEN analyzer, the appearance of emission occurs at potentials somewhat more positive than the location of the actual oxidation wave. Thus the reaction that generates the excited state A^* probably involves A^- and TPrA in a manner analogous to that proposed for HMC_3 [2] i.e.,

$$A + e \rightarrow A^- \quad (1)$$

$$A^- + Pr_3N \rightarrow Pr_3N^+ \quad (2)$$

$$Pr_3N^+ \rightarrow Pr_2NC^*HEt + H \quad (3)$$

$$Pr_2NC^*HEt + A^- \rightarrow + A^* + Pr_2NCHEt \quad (4)$$

$$A^* \rightarrow A + h\nu \quad (5)$$

In aqueous solutions A^- and its products are confined to the micellar phase.

The effect of IR144 concentration on ECL emission intensity is shown in Fig. 8. The background emission of TPrA is very weak (below 30 counts) compared to the ECL emission of IR144 down to micromolar levels (Fig. 8). The emission intensity is a strong function of scan direction. On the forward scan, as shown in Fig. 8, the luminescence rises as the catalytic current increases. However, the emission falls sharply, faster than expected from the diffusion-controlled consumption of reagents, after passing through the first wave. This is probably caused by the irreversible decomposition of A^- at the potential of the second wave. Thus on the reverse scan, the luminescence is extremely weak. The ECL intensity for IR144 in SDS surfactant solution was relatively weak when compared to the emission for IR144 in organic solvent, but still might be useful in analytical applications as a probe. The ECL intensity for IR125 under similar conditions was much weaker than that with IR144 (Fig. 9). This result for IR125 is consistent with its spectroscopic properties and weak fluorescence in both aqueous and surfactant solutions.

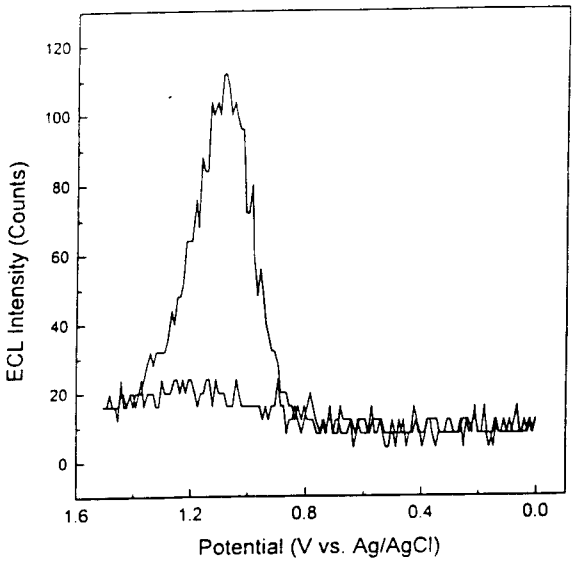

FIG. 9. ECL emission–potential transient of 2.0×10^{-4} M IR125 and 0.1 M TPrA in 0.1 M SDS solution. Scan rate, 0.05 V/s; 0.1 M sodium phosphate buffer, pH 7.3.

CONCLUSIONS

The spectroscopic properties of two tricarbocyanine dyes with the same heterocyclic nuclei (dimethyl naphthoindole), IR144 and IR125, were investigated. With IR144, the dimer is clearly evident from the absorption spectra in water when compared to those in MeOH. The absorption maximum is red-shifted (by about 54–57 nm) by the addition of surfactants above their CMC to the aqueous solvent. Both the dimer band at 701 nm in water and the monomer band at 741 nm in MeOH were observed.

In aqueous solution in the presence of SDS, oxidation waves of IR144 are observed at +0.62 and +0.86 V vs Ag/AgCl. The catalytic reaction between the

oxidation of IR144 and TPrA generated ECL in MeCN and aqueous SDS solutions. The ECL emission for IR125 is much weaker than that of IR144 in SDS surfactant solution due to the lower fluorescence efficiency of the compound. Thus, in aqueous surfactant solution, only IR144 is a candidate for analytical ECL applications.

ACKNOWLEDGMENTS

The support of this research by IGEN and the Robert A. Welch Foundation is gratefully acknowledged.

REFERENCES

1. T. C. Richards and A. J. Bard. Anal. Chem., 67, 3140 (1995).
2. S. K. Lee, M. M. Richter, L. Strekowski, and A. J. Bard. Anal. Chem., 69, 4126 (1997).
3. (a) S. A. Soper and Q. L. Mattingly, J. Am. Chem. Soc., 116, 3744 (1994). (b) H. Sato, M. Kawasaki, K. Kasatani, N. Nakashima, and K. Yoshihara, Bull. Chem. Soc. Jpn., 56, 3588 (1983). (c) S. P. Vlesco and G. R. Flemming, Chem. Phys., 65, 59 (1982).
4. J. Texter, in R. A. Mackay and J. Texter (Eds.), "Electrochemistry in Colloids and Dispersions", VCH Publishers, New York, 1992.
5. H. Sato, M. Kawasaki, and K. Kasatani, J. Phys. Chem., 87, 3759 (1983).
6. J. H. Fendler and E. J. Fendler, "Catalysis in Micellar and Macromolecular Systems," Academic Press, New York, 1975.
7. C. A. Bunton, L. S. Romsted, and G. Savelli, J. Am. Chem. Soc., 101, 1253 (1979).
8. N. Funasuki and S. Hada, J. Phys. Chem., 84, 736 (1980).
9. P. McCord and A. J. Bard, J. Electroanal. Chem., 91, 318 (1991).
10. W. West and B. H. Carrol, J. Chem. Phys., 19, 417 (1951).
11. G. Patonay, M. D. Antoine, S. Devanathan, and L. Strekowski, Appl. Spectrosc., 45, 457 (1991).
12. R. C. Benson and H. Kues, J. Chem. Eng. Data, 22, 379 (1977).

13. S. K. Rentsch, Chem. Phys., 69, 81 (1982).
14. A. J. Bard and L. R. Faulkner, "Electrochemical Methods", John Wiley & Sons, New York, 1980, pp. 215–227.
15. A. E. Kaifer and A. J. Bard, J. Phys. Chem., 89, 4876 (1985).
16. J. Ouyang and A. J. Bard, Bull. Chem. Soc. Jpn., 61, 17 (1988).
17. (a) Y. Ohawa, Y. Shimazaki, and S. Aoyagui, J. Electroanal. Chem., 114, 235 (1980). (b) G. L. McIntire, D. M. Chiappardi, R. L. Casselberry, and H. N. Blount, J. Phys. Chem., 86, 2632 (1982).

Received: May 27, 1998
Accepted: June 15, 1998